

Charge transport-mediated recruitment of DNA repair enzymes

Pak-Wing Fok,^{1,2} Chin-Lin Guo,³ and Tom Chou^{2,4}

¹*Applied and Computational Mathematics, California Institute of Technology, CA 91125*

²*Dept. of Biomathematics, UCLA CA 90095-1766**

³*Applied Physics and Bioengineering, California Institute of Technology, CA 91125*

⁴*Dept. of Mathematics, UCLA CA 90095-1766†*

(Dated: October 30, 2018)

Damaged or mismatched bases in DNA can be repaired by Base Excision Repair (BER) enzymes that replace the defective base. Although the detailed molecular structures of many BER enzymes are known, how they colocalize to lesions remains unclear. One hypothesis involves charge transport (CT) along DNA [Yavin, *et al.*, PNAS, **102**, 3546, (2005)]. In this CT mechanism, electrons are released by recently adsorbed BER enzymes and travel along the DNA. The electrons can scatter (by heterogeneities along the DNA) back to the enzyme, destabilizing and knocking it off the DNA, or, they can be absorbed by nearby lesions and guanine radicals. We develop a stochastic model to describe the electron dynamics, and compute probabilities of electron capture by guanine radicals and repair enzymes. We also calculate first passage times of electron return, and ensemble-average these results over guanine radical distributions. Our statistical results provide the rules that enable us to perform implicit-electron Monte-Carlo simulations of repair enzyme binding and redistribution near lesions. When lesions are electron absorbing, we show that the CT mechanism suppresses wasteful buildup of enzymes along intact portions of the DNA, maximizing enzyme concentration near lesions.

PACS numbers: 87.15.H,82.39.Pj,05.10.Gg,05.40.-a

I. INTRODUCTION

The genomes of all living organisms are constantly under attack by mutagenic agents such as reactive oxygen species and ionizing radiation. Such processes can damage bases giving rise to localized lesions in the DNA^{1,2} that can lead to harmful mutations and diseases such as cancer. For example, guanine residues can be oxidized, generating a radical called 7,8-dihydro-8-oxoguanine, or oxoG for short. Unlike the non-oxidized form, this radical can pair with both cytosine and adenine, ultimately giving rise to GC \rightarrow TA transversion mutations¹ upon multiple replications. Lesions can also arise through alkylation, hydration and deamination.¹

One defense mechanism against these mutation processes is the Base Excision Repair (BER) pathway. BER enzymes recognize and undo damage to DNA by adsorbing onto the sugar-phosphate backbone, locating the lesion and excising it. The biomechanical functions of repair enzymes have been well established and their 3D structures are known in great detail.³ There are four main types of BER enzyme: DNA glycosylases, AP-endonucleases, DNA polymerases and DNA ligases. Each of these enzymes has a different role in the BER family. For example, DNA glycosylases initiate the repair pathway, detecting and recognizing distinct forms of DNA damage while the endonucleases are responsible for cleaving the sugar-phosphate backbone. Together, these enzymes maintain the overall integrity of DNA, generally ensuring that miscoded proteins are kept to a minimum.

The problem of how a BER enzyme locates a lesion on DNA is a specific example of how enzymes find localized targets. The DNA of *E. coli* contains about 10^6

base pairs. If we assume that BER enzymes find lesions through a pure 1D diffusive “sliding” process with diffusion constant D base pairs²/ s , the search time is roughly $10^{12}/D$. Estimating D to be 5×10^6 base pairs²/ s , the value for a human DNA glycosylase,⁶ we obtain a search time of about $2 \times 10^5 s \approx 2$ days, much longer than even the reproductive period of *E. coli*. Therefore, it is likely that other mechanisms are responsible for DNA target location.

In 1970, Riggs *et al.*^{7,8} measured the association rate of the LacI repressor protein to its target on DNA to be about $10^{10} M^{-1} s^{-1}$. This was puzzling because the theoretical upper limit for the association rate of a LacI enzyme diffusing in 3D is predicted (via the Debye-Smoluchowski formula) to be about 2 orders of magnitude less. This fundamental biophysical problem was studied in the seminal work of von Hippel and co-workers^{9,10,11,12} and the “faster-than-diffusion” search of targets on DNA has received recent attention.^{13,14,15,16,17,18} Facilitated diffusion is one mechanism^{11,14,16,19} proposed to explain the accelerated search. Instead of diffusing directly to their target, the searching enzymes can spend part of their time attached to the DNA and perform a 1D random walk along part of the strand. If the enzyme is able to spend 50% of its time on the DNA and 50% of its time diffusing in 3D, and the diffusion constants in 1D and 3D are comparable, the association rate is predicted to increase by as much as 100 ,¹⁶ bringing it in line with the experiments in Riggs *et al.*^{7,8} However, other authors have shown that (i) typical enzymes are highly associated with DNA, spending over 99.999% of their time on the strand¹⁴ and (ii) the diffusion constant in 1D can be 1000 times smaller than in 3D,²⁰ resulting in a negligible reduction of the search

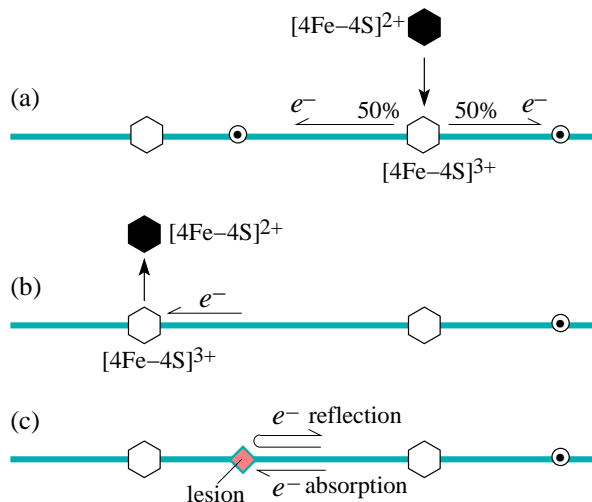


FIG. 1: Redox mechanism for repair enzyme interaction based on the papers by Yavin, *et al.*⁴ and Boon, *et al.*⁵ (a) A MutY in the 2+ state (solid hexagon) adsorbs and oxidizes to the 3+ state (empty hexagon) by releasing an electron along the DNA. The electron is emitted to the left or right of the enzyme with equal probability. Guanine radicals (circumscribed dots) can absorb electrons and prevent oxidation of nearby adsorbed enzymes. (b) A MutY repair enzyme in the 3+ state absorbs an electron and is reduced, causing it to desorb. (c) Lesions also prevent passage of electrons, either through electron absorption or reflection. In our analysis, lesions act differently from oxoG radicals in that they can continuously absorb electrons.

time. Hence, facilitated diffusion in its basic form is not adequate to explain the fast reaction rates observed. Extensions to the facilitated diffusion theory can incorporate finite enzyme concentrations,¹⁸ “antenna” effects resulting from the conformation of the DNA,¹⁷ fast inter-segment transfers of the protein,¹⁶ specific/non-specific protein-DNA interactions,¹⁶ and directed DNA sliding.²¹

Although BER enzymes may colocalize to lesions by exploiting the facilitated diffusion mechanisms cited above, other mechanisms are likely required for efficient and timely recruitment to lesions. A charge-transport (CT) mechanism has been recently proposed as a possible basis for efficient scanning by MutY, a type of DNA glycosylase.^{4,5} MutY is known to contain an iron-sulfur cluster which plays a key role in the CT mechanism. The cluster can take one of two forms: $[4Fe-4S]^{2+}$ and $[4Fe-4S]^{3+}$. When MutY is in solution, the cluster is in the 2+ state and is resistant to oxidation. However, upon binding to DNA, the cluster potential is shifted, making the 3+ state more accessible. The result is that after binding, MutY- $[4Fe-4S]^{2+}$ is easily oxidized and releases an electron along the DNA, as shown in Fig 1(a). It should be noted that the 3+ state of MutY has a binding affinity that is about 4 orders of magnitude larger than that of the 2+ state.²² Therefore MutY- $[4Fe-4S]^{2+}$ spends most of its time in solution whereas MutY- $[4Fe-4S]^{3+}$ exists

primarily adsorbed onto DNA.

Although controversial about 15 years ago, long range electron transport in DNA is now a well accepted phenomenon.^{23,24} Experiments indicate that charge transport can occur over 40Å (about 12 base pairs) in less than a nanosecond^{25,26} and the influence of DNA strand crossovers on CT is generally small.²³ Although electron dynamics along DNA is in general very complicated, some aspects of the process are now understood. For example, both guanine and adenine can act as carriers of positive charge; in analogy with semiconductors, oxidized DNA can transport charge via the transfer of holes from base to base.

Quantifying how BER enzymes adsorb to DNA and how they are recruited to lesions has so far been restricted to simple scaling arguments.²⁷ In this paper, in order to explore the implications of DNA target selection solely by CT, we assume that adsorbed MutY BER enzymes do not slide along the DNA. However, upon first attachment to DNA, the enzyme will emit an electron that propagates along the strand in a random direction and its cluster will go from the $[4Fe-4S]^{2+}$ to the $[4Fe-4S]^{3+}$ state. Should this electron become absorbed by another MutY- $[4Fe-4S]^{3+}$ enzyme further along the DNA, the 3+ form is reduced and desorbs (Fig 1(b)). If the electron back-scatters and returns to the original MutY, it self-desorbs. Although the model proposed in this paper is intended to specifically describe the colocalization and redistribution of MutY through the redox reaction of its iron-sulfur cluster, many BER enzymes, in fact, contain such a cluster, *e.g.* endonuclease III. Therefore, we think that our model may be more general and could also describe the binding kinetics of other enzymes.

Since unbiased stochastic motion in 1D always leads to return of the electron,²⁸ in the absence of any other electron absorbers on the DNA, a MutY BER enzyme that is deposited will eventually self-desorb with probability 1. However, BER enzymes can be recruited to DNA by preexisting electron absorbers. These are typically guanine radicals (“oxoG”) and other lesions, indicated in Fig. 1(c) by circumscribed dots and filled diamonds, respectively. It has been suggested that oxoG plays an important role in the seeding of MutY onto DNA.⁴ The oxoG radicals, like adsorbed enzymes, are able to absorb electrons, preventing them from returning and desorbing BER enzymes that originally released them. Therefore, the oxoG radical in Fig. 1(a) can absorb one left-moving electron and prevent it from back-scattering and desorbing the right-most enzyme. Upon reduction, oxoG radicals convert to normal guanine bases, no longer absorb electrons, and no longer take part in the CT mechanism.

Other lesions do not simply annihilate by absorbing electrons; rather, they require the physical presence of BER enzymes to excise them. These lesions may recruit smaller, more abundant proteins from solution that permit multiple electron absorption. Another possibility is that the lesions reflect electrons. Both cases are shown in Fig. 1(c). Therefore, our basic model consists of right

and left-moving electrons, guanine radicals, oxidized and reduced forms of BER enzymes, and lesions on the DNA strand. Newly adsorbed BER enzymes instantly release electrons (right or left-moving), while oxoG radicals, lesions, and oxidized BER enzymes absorb electrons and prevent their passage.

In this paper, we model the adsorption, desorption and redistribution of repair enzymes using the redox mechanism shown in Fig. 1. We first derive some exact results in the absence of any lesions; in particular, enzyme adsorption probabilities and the time taken for returning electrons to induce enzyme desorption. These results enable us to define rules for Monte-Carlo simulations of the dynamics of multiple enzymes. For electron absorbing lesions, simulations show that if enzymes are deposited onto a DNA at a rate that is slow compared to the electron dynamics, the distance between a lesion and the closest enzyme scales as $O(n^{-2/3})$ for large n , while total number of enzymes adsorbed between two lesions scales as $O(n^{1/3})$. However, because of the CT mechanism, this accumulation is not uniform along the DNA and the maximum enzyme density always occurs at lesions. Hence *for electron-absorbing lesions*, the CT mechanism concentrates enzymes to damaged bases in DNA, consistent with the qualitative predictions in Yavin, *et al.*⁴ and Boon, *et al.*⁵

The outline of this paper is as follows. In the next section, we develop a model for the electron dynamics based on the stochastic Broadwell model.^{29,30,31,32} Pairs of guanine radicals, BER enzymes or lesions define the boundary of a segment (a “gap”) over which an electron can propagate. Section III contains our results. In Section III A, we derive enzyme sticking probabilities and the time taken for returning electrons to desorb the enzymes that originally emitted them. In particular, we derive the MutY desorption rate in terms of the electron scattering (flip rate) and the electron speed. In Section III B, we perform implicit-electron Monte-Carlo simulations to study the redistribution and accumulation of enzymes between two fixed lesions on the DNA. Finally, in Section IV, we discuss facilitated recruitment of enzymes to lesions in the context of the CT hypothesis, as well as the biological advantages and disadvantages of the proposed CT mechanism.

II. STOCHASTIC CHARGE TRANSPORT MODEL

A. One-sided Broadwell problem

In analogy with Bicout’s analysis for the unrelated problem of microtubule growth dynamics,²⁹ we now present similar equations for the dynamics of electrons associated with repair enzymes. Consider Fig. 2(a): oxoG guanine radicals with density ρ are distributed randomly along an infinite strand of DNA. A single repair enzyme initially attaches to the DNA at a random position, in

Symbol	Definition	Units
P_+	Probability density of rightward electron	1/L
P_-	Probability density of leftward electron	1/L
X	Position along DNA	L
X_0	Position of electron release	L
T	Time	T
ρ	Density of oxoG guanine radicals on DNA	1/L
L	Distance between two oxoGs/enzymes	L
F	electron flip rate	1/T
V	Electron speed	L/T
M	Electron decay rate	1/T
k_{on}	Deposition rate of enzymes	1/(L · T)

TABLE I: Table of dimensional variables and parameters. The analysis performed assumes $M = 0$. L represents length and T represents time.

Symbol	Math defn.	Descriptive definition
Q_{\pm}	P_{\pm}/ρ	Rightward/ Leftward electron probability density
x	ρX	Coordinate along DNA
x_0	ρX_0	Position of electron release
t	ρVT	Time
ℓ	ρL	“Gap size” : distance between two oxoGs/enzymes/lesions
f	$F/\rho V$	Electron flip rate
μ	$M/\rho V$	Electron decay rate
ξ	-	Position of enzyme adsorption
d_1, d_2	-	Enzyme-lesion/enzyme-enzyme distance (see Fig. 6)

TABLE II: Definitions of dimensionless symbols in terms of the dimensional quantities in Table I.

between two electron absorbing oxoGs. The enzyme immediately emits an electron along the DNA to the left or right with equal probability. The electron can only move with speed V , in the positive or negative X -directions, executing random flips between the two directions with rates F . Furthermore, emitted electrons can be annihilated with rate M through nonspecific interactions with random electron absorbers diffusing in the bulk.

In general, two steps are required for a MutY enzyme to bind to DNA. First, when MutY-[4Fe-4S]²⁺ is in contact with the DNA, it has to undergo oxidation by releasing an electron. The oxidized form of the enzyme binds more strongly to DNA. Second, the released electron must be absorbed by some particle other than the enzyme (an oxoG, an already adsorbed MutY or a lesion) to prevent it from returning and reducing the enzyme. This allows the enzyme binding to become “permanent”. Therefore the net binding probability depends on (i) the probability of electron release by MutY-[4Fe-4S]²⁺ (when

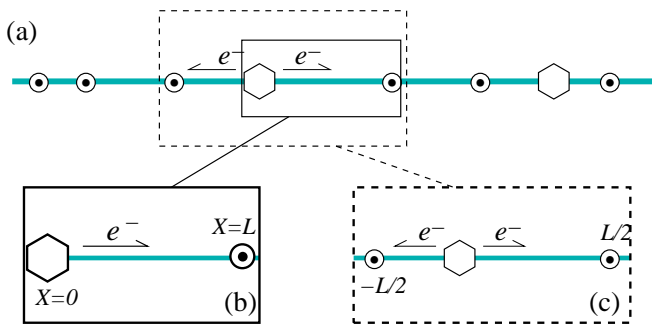


FIG. 2: (a) A repair enzyme (hexagon) adsorbs onto a DNA which is initially populated by guanine radicals (circled dots) with a density ρ . An electron is emitted to the left or right with equal probability. The emitted electron has flip rate F , speed V , and decay rate M . (b) The one-sided Broadwell problem. An electron is emitted from $X = 0$ with probability 1 toward a guanine radical at $X = L$. (c) The two-sided Broadwell problem. An enzyme is deposited between two guanine radicals which are a distance L apart. Immediately after landing inside this segment, an electron is emitted to the left or right with equal probability.

in contact with the DNA) and (ii) how far neighboring electron absorbers are from the adsorbed MutY. In this paper, we assume that when enzymes adsorb onto the DNA, they *always* oxidize, releasing an electron with probability 1; in Fig. 2(b), the electron is released to the right with probability 1 and in Fig. 2(c), the electron is released to the left or right with probability $1/2$. In principle, an enzyme can attach to and then immediately detach from the DNA without releasing its electron, but assuming the electron release rate is large, we neglect this process. The adsorption probabilities we derive later in this section will depend only on the gap size L and the parameters for electron motion.

Finally, we assume that the DNA is immersed in an infinite reservoir of enzymes which is kept at a fixed chemical potential. The rate of deposition of enzymes onto the DNA is assumed to be constant. A deposited enzyme can either adsorb by having its released electron captured by neighboring electron absorbers or it can desorb due to its electron returning.

To build our full solution, we first derive exact analytical expressions for the “one-sided” problem shown in Fig. 2(b) which consists of an enzyme at $X = 0$ and a guanine radical at $X = L$. At time $T = 0$, an electron is emitted from a position $X_0 > 0$ (subsequently, we will take the limit $X_0 \rightarrow 0$) with speed V in the positive X -direction. For the one-sided problem, the electron is emitted only to the right. The probability that the electron is at a position between X and $X + dX$ at time T , and moving to the right with velocity V is denoted $P_+(X, T)$. Similarly, $P_-(X, T)$ denotes the probability density of an electron moving with speed V in the negative X -direction. The electron can flip directions by scattering from inhomogeneities and thermally excited conformational variations

along the DNA.^{33,34} We model this flipping process as a spatially homogeneous process occurring with constant rate F , independent of any structure along the DNA such as base pair sequence.

The evolution equations for the probability densities $P_{\pm}(X, T)$ are

$$\begin{aligned} \frac{\partial P_+}{\partial T} &= -V \frac{\partial P_+}{\partial X} - FP_+ + FP_- - MP_+, \\ \frac{\partial P_-}{\partial T} &= V \frac{\partial P_-}{\partial X} + FP_+ - FP_- - MP_- \end{aligned} \quad (1)$$

where $0 \leq X \leq L$. Eqs. (1) describe the probability density of electrons being advected to the right and left. The flipping of the electron motion is represented through F and couples the equations for P_+ and P_- . Furthermore, the densities decay in time with an annihilation rate M . Electrons can be annihilated by being absorbed by other proteins (besides BER enzymes) in solution. If these proteins adsorb onto the DNA, absorb an electron and desorb back into solution, an electron is permanently removed from the DNA.

The boundary conditions and initial conditions are

$$P_+(0, T) = P_-(L, T) = 0, \quad (2)$$

$$P_+(X, 0) = \delta(X - X_0), \quad (3)$$

$$P_-(X, 0) = 0. \quad (4)$$

The boundary conditions (2) arise because the enzyme at $X = 0$ and the oxoG at $X = L$ (see Fig. 2(b)) are both perfect electron absorbers. When $X_0 \rightarrow 0$, the initial condition (3) reflects the fact that an electron is released to the right from the enzyme at $X = 0$. Initially, there are no leftward traveling electrons in Fig. 2(b), justifying Eq. (4). All variable and parameters are listed in Tables I.

We now define dimensionless independent variables through the guanine radical density ρ and the rightward electron travel time $1/(\rho V)$:

$$x = \rho X, \quad t = \rho VT, \quad (5)$$

so that Eqs. (1) can be written in the form

$$\frac{\partial \mathbf{Q}}{\partial t} = \mathbf{L} \mathbf{Q}, \quad \mathbf{Q} = \begin{pmatrix} Q_+(x, t) \\ Q_-(x, t) \end{pmatrix}, \quad (6)$$

where $Q_{\pm} = P_{\pm}/\rho$ and

$$\mathbf{L} = \begin{bmatrix} -\frac{\partial}{\partial x} - f - \mu & f \\ f & \frac{\partial}{\partial x} - f - \mu \end{bmatrix}, \quad (7)$$

and $0 \leq x \leq \ell \equiv \rho L$. In Eq. (7),

$$f = \frac{F}{\rho V}, \quad \mu = \frac{M}{\rho V}, \quad (8)$$

is the dimensionless flipping rate and electron decay rate. The boundary and initial conditions (2), (3), (4) become

$$\begin{aligned} Q_+(0, t) = Q_-(\ell, t) &= 0, \\ Q_+(x, 0) &= \delta(x - x_0), \\ Q_-(x, 0) &= 0, \end{aligned} \quad (9)$$

where $x_0 = \rho X_0$. In the physical problem, an electron is released from the enzyme as soon as it initially attaches to the DNA. Therefore, we solve Eqs. (6) with (7) and (9) taking the limit $x_0 \rightarrow 0$ (for details, see Appendix A). The dimensionless variables are tabulated and defined in Table II. Henceforth all of our results and analyses will be presented for $\mu = 0$.

The probability of the enzyme in Fig. 2(b) self-desorbing before time t is given by $\int_0^t Q_-(0, t') dt'$ where Q_- can be found by taking the inverse Laplace Transform of Eq. (A4) in Appendix A. Therefore, the enzyme desorption and sticking probabilities for the one-sided problem are

$$\frac{f\ell}{1+f\ell} \quad \text{and} \quad 1 - \frac{f\ell}{1+f\ell} = \frac{1}{1+f\ell}, \quad (10)$$

respectively.

B. Two-sided Broadwell problem

Now consider the two-sided problem depicted in Fig. 2(c). A repair enzyme lands at position ξ between two oxoG guanine radicals that are a distance ℓ apart. The solution to the full problem can be found by splitting it into two subproblems and using our results from Section II A. Instead of solving for the densities on $[0, \ell]$, we can solve for Q_\pm separately on $[\xi, \ell/2]$ (with the enzyme initially deposited at ξ and the guanine radical at $\ell/2$), on $[\xi, -\ell/2]$ (with the enzyme at ξ and the guanine radical at $-\ell/2$) and combine the results. The enzyme desorption and adsorption probabilities (10) extend straightforwardly:

$$\begin{aligned} \Pi_{\text{desorb}}(\xi, \ell) &= \frac{1}{2} \left[\frac{f(\frac{\ell}{2} - \xi)}{1 + f(\frac{\ell}{2} - \xi)} + \frac{f(\frac{\ell}{2} + \xi)}{1 + f(\frac{\ell}{2} + \xi)} \right], \\ \Pi_{\text{adsorb}}(\xi, \ell) &= \frac{1}{2} \left[\frac{1}{1 + f(\frac{\ell}{2} - \xi)} + \frac{1}{1 + f(\frac{\ell}{2} + \xi)} \right]. \end{aligned} \quad (11)$$

A plot of the sticking probability Π_{adsorb} for different values of f and for two different gap sizes is shown in Fig. 3. For a fixed gap size, and sufficiently large f (corresponding to a diffusive electron motion), permanent BER enzyme adsorption is less likely to occur near the center of the gap because absorption of the electron by guanine radicals is less likely to occur. The permanent adsorption or sticking probability is more uniform when f is small (corresponding to a ballistic electron motion): whether the oxoG radical is close or far away from the

Symbol	Descriptive definition	See Eq.
$\Pi_{\text{adsorb}}(\xi, \ell)$	Enzyme adsorption probability	(11)
$\Pi_{\text{desorb}}(\xi, \ell)$	Enzyme desorption probability	(11)
$\bar{\Pi}_{\text{adsorb}}(\ell)$	Enzyme adsorption prob. averaged over landing position ξ	(12)
$\bar{\Pi}_{\text{desorb}}(\ell)$	Enzyme desorption prob. averaged over landing position ξ	(20)
$\langle \bar{\Pi}_{\text{adsorb}} \rangle$	Enzyme adsorption prob. averaged over landing posn. ξ and gap size ℓ	(14,16)
t_r	Random variable for conditional return time of electron	(17)
$\tau_r(\xi, \ell)$	Mean conditional return time (MCRT) of an electron	(18)
$\bar{\tau}_r(\ell)$	MCRT of an electron averaged over landing position ξ	(19)
$\langle \bar{\tau}_r \rangle$	MCRT of an electron averaged over landing posn. ξ and gap size ℓ	(21)

TABLE III: Derived adsorption/desorption probabilities, electron return times and related quantities.

enzyme makes little difference to the adsorption probability. Finally, for fixed f , increasing the gap size decreases the adsorption probability because guanine annihilation by the electron is less likely to occur. The diffusive and ballistic behaviors of the Broadwell model are derived in Appendix B.

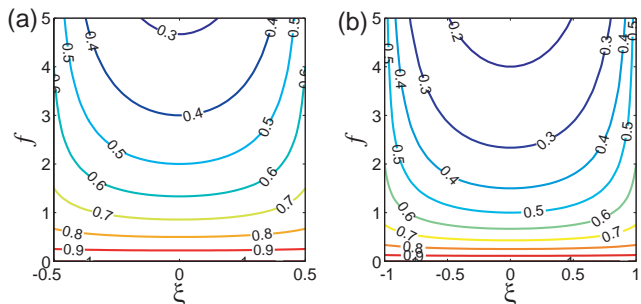


FIG. 3: Dependence of enzyme sticking probability, Π_{adsorb} (see Eq. (11)), on dimensionless flip rate f and landing position $-\ell/2 < \xi < \ell/2$, for the deposition of a single enzyme into a gap (the segment of DNA between two guanine radicals) of size ℓ . (a) $\ell = 1$ with radicals located at ± 0.5 (b) $\ell = 2$ with radicals located at ± 1 .

III. RESULTS AND DISCUSSION

A. Statistics of repair enzymes away from lesions

In this section, we present and discuss deposition statistics that are valid far away from lesions. First, using Eq. (11), we average over the landing position ξ to calculate mean sticking/adsorption probabilities of

repair enzymes that are deposited between two guanine radicals that are a distance ℓ apart. The inter-radical distances (“gaps”) in DNA will, in general, be randomly distributed. Therefore we ensemble-average our results over the distribution that ℓ is expected to obey. Second, we find the mean return times of electrons, *i.e.* the time taken for a deposited enzyme to be desorbed by its own electron, providing it desorbs. Again, our results are ensemble-averaged over randomly distributed gap sizes. The quantities we shall compute and analyze in this section are listed in Table III.

All the results presented are for *adiabatic* depositions. A deposition is adiabatic if the inter-deposition time is much larger than the time scale of the electron dynamics. In other words, for every enzyme deposited, its released electron completes its motion before the deposition of the next enzyme. At any given time, there is at most one traveling electron on the DNA. For details, see Appendix C.

1. Repair enzyme sticking probability

One quantity of interest is the probability that any given repair enzyme that lands on the DNA will not be kicked off by its own electron, and will remain adsorbed. Enzyme sticking relies on efficient capture of the released electron by neighboring electron absorbers (guanine radicals and adsorbed enzymes). Intuitively, one would expect that a greater density of absorbers with smaller gaps would result in a more efficient capture of enzymes.

For a single repair enzyme deposited onto the DNA, landing at a position $-\ell/2 < \xi < \ell/2$ (see Fig. 2(c)) inside a gap of length ℓ , centered about $x = 0$, the probability of it remaining on the DNA is given by Π_{adsorb} in Eq. (11). This quantity can be averaged over all possible deposition positions ξ within the gap to obtain

$$\begin{aligned} \bar{\Pi}_{\text{adsorb}} &= \frac{1}{2\ell} \int_{-\ell/2}^{\ell/2} \left[\frac{1}{1 + f(\frac{\ell}{2} - \xi)} + \frac{1}{1 + f(\frac{\ell}{2} + \xi)} \right] d\xi \\ &= \frac{2}{f\ell} \tanh^{-1} \left(\frac{f\ell}{2 + f\ell} \right). \end{aligned} \quad (12)$$

This result is plotted in Fig. 4 (dashed line). Eq. (12) gives the sticking probability of a repair enzyme newly deposited between two electron absorbers separated by ℓ , *uniformly averaged* over its deposition position within the gap.

We now average over the gap length distribution to compute the sticking probability for deposited enzymes that land anywhere along the entire DNA strand. For an infinite, lesion free DNA, depositing an enzyme will, in general, change the local guanine and enzyme distribution. Hence, the sticking probabilities will also change with each successive deposition, making the calculation difficult in the context of the Broadwell model. However it is possible to calculate the sticking probability for a

given gap distribution. In special cases where this distribution is known or simple to calculate, we can compute the efficiency of enzyme recruitment onto the DNA.

Consider the case of a DNA with a discrete distribution of gaps $\ell_1, \ell_2, \ell_3, \dots$. Suppose that on the DNA, a fraction ϕ_j of the gaps have size ℓ_j . Now consider many realizations of a single enzyme deposited onto this DNA. The fraction of enzymes that lands in gaps of size ℓ_j is $\phi_j \ell_j / \sum_{j=1}^{\infty} \phi_j \ell_j$ and the fraction of these that stays adsorbed, using Eq. (12), is

$$\frac{2 \phi_j \tanh^{-1} \left(\frac{f\ell_j}{2 + f\ell_j} \right)}{f \sum_{j=1}^{\infty} \phi_j \ell_j}. \quad (13)$$

The fraction of enzymes that stays adsorbed (in any gap) is obtained by summing over j . In the continuum limit, $\ell_j \rightarrow \ell$, $\phi_j \rightarrow \phi(\ell)d\ell$, where ℓ is the continuous gap length and $\phi(\ell)$ is the probability distribution function (PDF) for ℓ . We obtain

$$\langle \bar{\Pi}_{\text{adsorb}} \rangle = \frac{2}{f\langle \ell \rangle} \int_0^{\infty} \phi(\ell) \tanh^{-1} \left(\frac{f\ell}{2 + f\ell} \right) d\ell. \quad (14)$$

Note that $\langle \bar{\Pi}_{\text{adsorb}} \rangle \neq \int_0^{\infty} \phi(\ell) \bar{\Pi}_{\text{adsorb}}(\ell) d\ell$, the result that one might expect by naively averaging Eq. (12) over the gap distribution.

Since $\phi(\ell)$ depends on the number of enzymes deposited, it is time dependent. In principle, one could calculate how $\phi(\ell)$ changes as enzymes are adiabatically deposited. The corresponding evolution of the sticking probability is then given by Eq. (14). One possible way of finding how $\phi(\ell)$ evolves is to use a mean field theory for the particle distributions, but we leave this as the subject of a future investigation.

In the special case where one enzyme is deposited onto a DNA that only has guanine radicals, we can calculate $\phi(\ell)$ and hence $\langle \bar{\Pi}_{\text{adsorb}} \rangle$ explicitly. If the guanine radicals have a number density ρ , then the gap lengths, on average, are $1/\rho$, which corresponds to a unit dimensionless gap size (see Eq. (5)). Hence $\langle \ell \rangle = 1$ and the dimensionless gap sizes, Y , are exponentially distributed (see Appendix D) according to

$$\text{Prob}(\ell < \text{gap size} < \ell + d\ell) = e^{-\ell} d\ell, \quad (15)$$

so we set $\phi(\ell) = e^{-\ell}$. Substituting this result into Eq. (14), we obtain

$$\langle \bar{\Pi}_{\text{adsorb}} \rangle = \frac{e^{1/f} \text{Ei}(1/f)}{f}, \quad (16)$$

where $\text{Ei}(x) = \int_x^{\infty} \frac{e^{-t}}{t} dt$ is the exponential integral. This analytic result is plotted in Fig. 4 (solid line) and is confirmed by Monte-Carlo simulations (circles). The sticking probability increases when either the electron-absorber density ρ increases, the electron velocity V increases or the flip rate F decreases.

Equation (16) is valid only when the number of enzymes that have stuck is much less than the initial number of oxoG radicals. In this limit, the distribution of

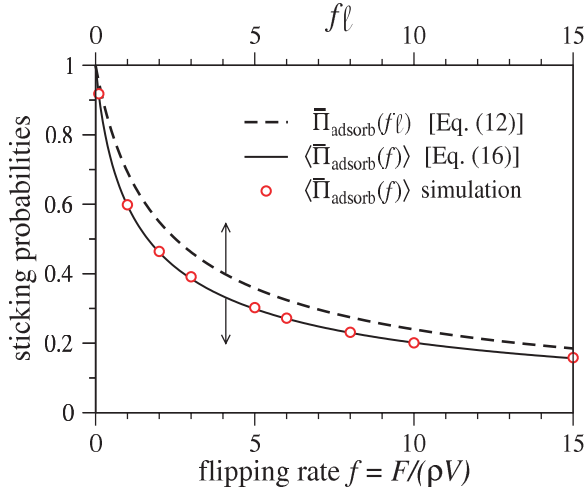


FIG. 4: Enzyme sticking probabilities as a function of dimensionless flip rate f . The simulation data was obtained by performing single depositions onto a DNA of length 100 (*i.e.*, with physical length $100/\rho$). The fraction of enzymes that remain on the DNA after performing 10^5 trials was recorded. Increasing the DNA length did not significantly affect the simulation results.

gap lengths will remain approximately exponential. For the human genome of $\sim 10^9$ base pairs, there are approximately 10^4 oxoGs present at any given time.³⁵ In this case, we expect that Eq. (16) should be fairly accurate for about the first dozen depositions.

Note that $\bar{\Pi}_{\text{adsorb}}$ (Eq. (12)) with $\ell = 1$ gives the

enzyme sticking probability inside an inter-radical gap of unit length, whereas $\langle \bar{\Pi}_{\text{adsorb}} \rangle$ (Eq. (16)) gives the enzyme sticking probability averaged over exponentially distributed inter-radical gaps lengths, but with unit mean. Intuitively, one would expect the boundaries defining the smaller gaps to be more efficient at sequestering electrons than those associated with larger gaps. However, the enhanced electron trapping by smaller gaps, leading to otherwise increased sticking probabilities is compensated by a higher deposition flux into larger gaps (large gaps collect more enzymes than small gaps). The net result of averaging over exponentially distributed gap sizes is for the larger gaps to dominate and lower the overall gap-averaged sticking probability. This is shown in Fig. 4 where for all values of f , $\langle \bar{\Pi}_{\text{adsorb}} \rangle < \bar{\Pi}_{\text{adsorb}}$ when $\ell = 1$.

2. Mean conditional return time of electrons

We now find the mean time that a BER enzyme stays on the DNA after its initial deposition, conditioned on its own electron returning and knocking the enzyme off. This quantity allows us to estimate a rate of desorption that can be used in more coarse-grained, higher level descriptions of the CT mechanism.

Consider depositing an enzyme into a gap of size ℓ at a position ξ satisfying $-\ell/2 < \xi < \ell/2$. The probability that the electron (e^-) returns in a time $t_r < t$, given that it returns is,

$$\begin{aligned} \text{Prob}(t_r < t \mid e^- \text{ returns}) &= \frac{\text{Prob}(t_r < t)}{\text{Prob}(e^- \text{ returns})} \\ &= \frac{\text{Prob}(t_r < t \mid e^- \text{ shoots right}) + \text{Prob}(t_r < t \mid e^- \text{ shoots left})}{\text{Prob}(e^- \text{ returns} \mid e^- \text{ shoots right}) + \text{Prob}(e^- \text{ returns} \mid e^- \text{ shoots left})} \\ &= \frac{\frac{1}{2} \int_0^t Q_-(x=0, t'; 0, \ell/2 - \xi) dt' + \frac{1}{2} \int_0^t Q_-(x=0, t'; 0, \ell/2 + \xi) dt'}{\frac{1}{2} \int_0^\infty Q_-(x=0, t'; 0, \ell/2 - \xi) dt' + \frac{1}{2} \int_0^\infty Q_-(x=0, t'; 0, \ell/2 + \xi) dt'}. \end{aligned} \quad (17)$$

In Eq. (17), $Q_-(x, t; x_0, \ell)$ is the leftward electron density at position $0 < x < \ell$ at time t given that the electron was released from $x = x_0$ at $t = 0$ (see Fig. 1(b) for the $x_0 = 0$ case). This density comes from solving Eqs. (6) and (7) along with the conditions (9).

The mean conditional electron return time τ_r can then be computed from

$$\tau_r(\xi; \ell, f) = \int_0^\infty t \frac{\partial}{\partial t} \text{Prob}(t_r < t \mid e^- \text{ returns}) dt. \quad (18)$$

Using Eq. (17), $\tau_r(\xi; \ell, f)$ in Eq. (18) can be found in terms of the Laplace-transformed density $\tilde{Q}_\pm(x, s)$ which

is given in Eq. (A4) of Appendix A. Upon averaging $\tau_r(\xi; \ell, f)$ over the initial landing positions ξ , we obtain

$$\begin{aligned} \bar{\tau}_r(\ell, f) &= \frac{2}{3f} \frac{3 + f\ell}{\sqrt{f\ell(2 + f\ell)}} \tanh^{-1} \left(\frac{\sqrt{f\ell}}{\sqrt{2 + f\ell}} \right) \\ &\quad + \frac{1}{3f} [f\ell - 1 - \frac{2}{f\ell} \log(1 + f\ell)]. \end{aligned} \quad (19)$$

We plot $\bar{\tau}_r(\ell, f)$, and validate Eq. (19) using MC simulations in Fig. 5(a). Finally, we further ensemble-average $\bar{\tau}_r$ over gap lengths ℓ . Consider many realizations of the deposition of a single enzyme onto an infinite DNA with

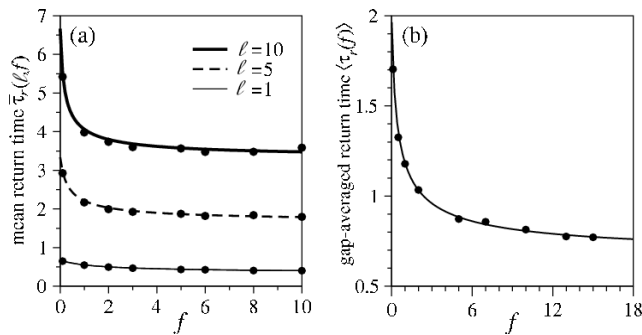


FIG. 5: (a) For adiabatic enzyme depositions into a gap of size ℓ , $\bar{\tau}_r$, the mean conditional return time of an electron, averaged over the enzyme landing position ξ , is recorded for different gap sizes and dimensionless flip rates f . The symbols represent data from Monte Carlo simulations and the solid line represents the analytic expression from Eq. (19). (b) For random, uniform, adiabatic enzyme depositions onto a DNA with randomly and uniformly distributed guanine radicals, $\langle \bar{\tau}_r \rangle$ as predicted by Eq. (21) is plotted as a function of the dimensionless flip rate f .

oxoGs whose gaps are exponentially distributed. The average time that the enzyme stays adsorbed, given that its electron eventually returns to knock it off, is $\langle \bar{\tau}_r \rangle$. The calculation of $\langle \bar{\tau}_r \rangle$ is similar to that of $\langle \bar{\Pi}_{\text{adsorb}} \rangle$ described in Section III A 1, but modified to account for the fact that the number of enzymes that self-desorb (*i.e.*, the number of return times that are finite) depends on ℓ . If an enzyme is deposited into a gap of size ℓ , the probability of self-desorbing after a finite time is given by (see Eq. (12))

$$\bar{\Pi}_{\text{desorb}}(\ell, f) = 1 - \frac{2}{f\ell} \tanh^{-1} \left(\frac{f\ell}{2 + f\ell} \right). \quad (20)$$

Therefore, the required expression for $\langle \bar{\tau}_r \rangle$ is

$$\langle \bar{\tau}_r(f) \rangle = \frac{\int_0^\infty \bar{\Pi}_{\text{desorb}}(\ell, f) \bar{\tau}_r(\ell, f) \ell e^{-\ell} d\ell}{\int_0^\infty \bar{\Pi}_{\text{desorb}}(\ell, f) \ell e^{-\ell} d\ell} \quad (21)$$

In the numerator of Eq. (21), $\bar{\Pi}_{\text{desorb}}(\ell, f) \ell e^{-\ell} d\ell$ is the fraction of deposited enzymes that (i) land in a gap that has a length between ℓ and $\ell + d\ell$ and (ii) eventually self-desorb after finite time. In the denominator, $\int_0^\infty \bar{\Pi}_{\text{desorb}}(\ell, f) \ell e^{-\ell} d\ell$ is the fraction of deposited enzymes that self-desorb after a finite time. The result (21) is confirmed by simulation data in Fig. 5(b).

Equation (21) was derived by considering the deposition of a single enzyme onto an infinite DNA with exponentially distributed gap lengths. However, as is the case with Eq. (16), it is also approximately true for a small number of depositions onto a finite DNA: providing the number of oxoGs annihilated is small compared to the total number of oxoGs, the distribution of gap lengths is

still approximately exponential. Hence, for a given deposition rate of enzymes *per unit length* onto an infinite DNA, Eq. (21) will hold approximately for times such that the fraction of oxoGs annihilated is small.

Given a deposition rate of enzymes (per unit length), we can estimate a desorption rate (per unit length) from Eq. (21). If desorption were a Poisson process, then the desorption rate, k_{off} , is found from the inverse of the mean unbinding time of the repair enzyme. Although the desorption process in our model depends on the dynamics of electron charge transport (rendering it to be non-Poisson), the inverse of the ensemble averaged conditional return time of an electron $1/\langle \bar{\tau}_r \rangle$, is nonetheless a reasonable definition for the detachment rate k_{off} . We expect this value of k_{off} to be accurate, as long as the fraction of oxoGs annihilated by repair enzymes is small. The probabilities and times relevant to electron dynamics are summarized in Table III.

B. Colocalization of enzymes to lesions

We now consider a permanent lesion on the DNA (one that does not annihilate upon absorption of an electron). Such a lesion may be bound to other enzymes and cofactors so that it can act as a sink for multiple electrons, or it can reflect electrons. In this section, we consider lesions that can either absorb or reflect electrons, as shown in Fig. 1(c). We are primarily interested in the average number of depositions required for a repair enzyme to be adsorbed within a certain (small) distance from the lesion.

For the sequential deposition of many enzymes onto a DNA populated with guanine radicals and lesions, the evolution of enzyme and guanine densities is not amenable to exact analytical solution. Therefore, our approach will be to track enzyme-lesion distances and enzyme concentrations on the DNA by performing Monte-Carlo simulations.

Each simulation consists of a series of adiabatic depositions. A deposition is simply the spontaneous appearance of a MutY-[4Fe-4S]³⁺ enzyme at a randomly chosen position along the DNA. Note that a deposition is an *attempted* adsorption: it can result either in the enzyme sticking to the DNA, or desorbing from it. In our simulations, the number of enzymes on the DNA can grow without bound. We do not model the bulk dynamics for MutY-[4Fe-4S]²⁺ enzymes in solution.

In our model, each enzyme that is deposited releases an electron along the DNA. However, rather than performing time-consuming, explicit simulations of a Broadwell process, we exploit our analytic results to implicitly account for the electrons. The rules for enzyme desorption and adsorption come from the probabilities $\bar{\Pi}_{\text{desorb}}$ and $\bar{\Pi}_{\text{adsorb}}$ found in Eqs. (11). Specifically, consider the deposition of an enzyme, E , between two already adsorbed enzymes, E_1 and E_2 (see Fig. 6(a)). Let the distance from E to E_i be d_i , $i = 1, 2$. Then the probability of E

adsorbing and knocking off E_i is $\frac{1}{2} \frac{1}{1+fd_i}$ and the probability of E self-desorbing is $\frac{1}{2} \left(\frac{fd_1}{1+fd_1} + \frac{fd_2}{1+fd_2} \right)$. In the case where an enzyme is deposited between a lesion and an adsorbed enzyme (see Fig. 6(b)), the adsorption and desorption probabilities have to be modified. If E_1 is replaced by an electron-reflecting lesion, the probability of E permanently adsorbing without displacing E_2 is zero. The probability of E adsorbing and knocking off E_2 is $\frac{1}{2} \frac{1}{1+fd_1}$ and the probability of self-desorption is $\frac{1}{2} + \frac{1}{2} \frac{fd_1}{1+fd_1}$. If E_1 is replaced by an electron-absorbing le-

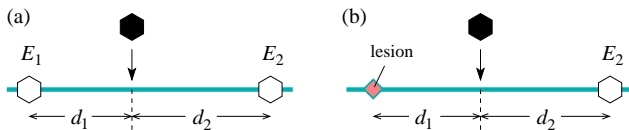


FIG. 6: (a) Deposition of new enzyme E (solid hexagon) in between two adsorbed enzymes E_1 and E_2 (empty hexagons). (b) Deposition of a new enzyme E between a lesion and an adsorbed enzyme, E_2 . Adsorption and desorption probabilities are given in Tables IV and V.

sion, the probability of E permanently adsorbing without displacing E_2 is $\frac{1}{2} \frac{1}{1+fd_1}$, the probability of E adsorbing and knocking off E_2 is $\frac{1}{2} \frac{1}{1+fd_2}$ and the probability of self-desorption is $\frac{1}{2} \left(\frac{fd_1}{1+fd_1} + \frac{fd_2}{1+fd_2} \right)$. These probabilities are summarized in Tables IV and V.

Event:	E self-desorbs	E adsorbs, E_1 desorbs	E adsorbs, E_2 desorbs
Probability:	$\frac{1}{2} \left(\frac{fd_1}{1+fd_1} + \frac{fd_2}{1+fd_2} \right)$	$\frac{1}{2} \frac{1}{1+fd_1}$	$\frac{1}{2} \frac{1}{1+fd_2}$

TABLE IV: Adsorption and desorption probabilities in Fig. 6(a) when the enzyme E is deposited between enzymes E_1 and E_2 .

Event:	E self-desorbs	E adsorbs, E_2 stays adsorbed	E adsorbs, E_2 desorbs
Probability: (reflecting lesion)	$\frac{1}{2} + \frac{1}{2} \left(\frac{fd_2}{1+fd_2} \right)$	0	$\frac{1}{2} \frac{1}{1+fd_2}$
Probability: (absorbing lesion)	$\frac{1}{2} \left(\frac{fd_1}{1+fd_1} + \frac{fd_2}{1+fd_2} \right)$	$\frac{1}{2} \frac{1}{1+fd_1}$	$\frac{1}{2} \frac{1}{1+fd_2}$

TABLE V: Adsorption and desorption probabilities in Fig. 6(b) when the lesion is an electron absorber and reflector.

MC simulations were performed on a periodic domain of size Γ containing a single lesion, which is equivalent to a single finite domain with length Γ and lesions at $x = 0$ and $x = \Gamma$. We start our simulations with no adsorbed BER enzyme (MutY), but with a unit density of guanine radicals (oxoG) whose gaps follow an exponential distribution (see Eq. (15)). When a single enzyme

is deposited randomly on $[0, \Gamma]$, the positions of the two particles (either oxoGs, lesions or already adsorbed enzymes) on either side are recorded and d_1 and d_2 are calculated (see Fig. 6). Using the probabilities in Tables IV and V, the outcome of this deposition event is determined: either the newly deposited enzyme adsorbs, or it desorbs due to its electron returning. Note that if an adsorption occurs, exactly one of three other events also has to occur: (i) a neighboring enzyme is reduced and desorbs (ii) a neighboring oxoG is annihilated or (iii) an electron is absorbed by a neighboring lesion.

Figure 7 shows density profiles obtained from our MC simulations. In Fig. 7(a), the depletion of guanine radicals is greater away from lesions: a guanine radical that is close to a lesion can, essentially, only be annihilated from one side. Near $x = 0$, the probability of oxoGs being annihilated from the left by a rightward-moving electron is very small. Similarly, near $x = 5$, the probability that oxoGs are annihilated from the right by leftward-moving electrons is also very small.

Figure 7(b) shows that electron reflecting lesions eventually prevent the build up of enzymes near lesions. The presence of an electron-reflecting lesion increases the local self-desorption rate. Note that the enzyme self-desorption probability is always greater in Fig. 6(b) than it is in Fig. 6(a) – when the lesion is electron reflecting. Therefore, near a reflecting lesion, the recruitment of enzymes by guanine radicals has to compete with this increased self-desorption rate. Although the density near the lesion increases with time, for a fixed time, its value is always smaller than the bulk value. Another way to understand the enzyme depletion is through a particle conservation argument. Since the total number of guanine radicals and BER enzymes is conserved, an increase in oxoG density near the boundaries must correspond to a decrease in the enzyme density.

Figures 7(c) and 7(d) show density profiles near electron-absorbing lesions. The oxoG densities in Fig. 7(c) remain essentially unchanged from those surrounded by electron-reflecting lesions (Fig. 7(a)). As shown in Figs. 7(b) and 7(d), the BER enzyme density profiles are also similar for a small number of depositions, away from lesions. On the other hand, 7(d) also shows that for larger deposition numbers, the BER enzyme density near electron-absorbing lesions increases markedly.

The total number of particles on the DNA strand can be found by integrating the densities from $x = 0$ to $x = \Gamma$. For example, in Fig. 7(b), the solid curve representing the enzyme density after one attempted deposition takes the value ~ 0.12 over most of the domain and decreases slightly near the lesions. Therefore the (average) number of enzymes that remain adsorbed after one attempted deposition is approximately $0.12 \times 5 = 0.6$. This is in excellent agreement with the solid curve in Fig. 4 and Eq. (16) for $f = 1$ since $\langle \bar{\Pi}_{\text{adsorb}} \rangle = e\text{Ei}(1) = 0.596\dots$

Figure 7 only shows the densities up to 20 deposition attempts. When the number of depositions is much greater than 20, all of the enzyme-seeding guanine radi-

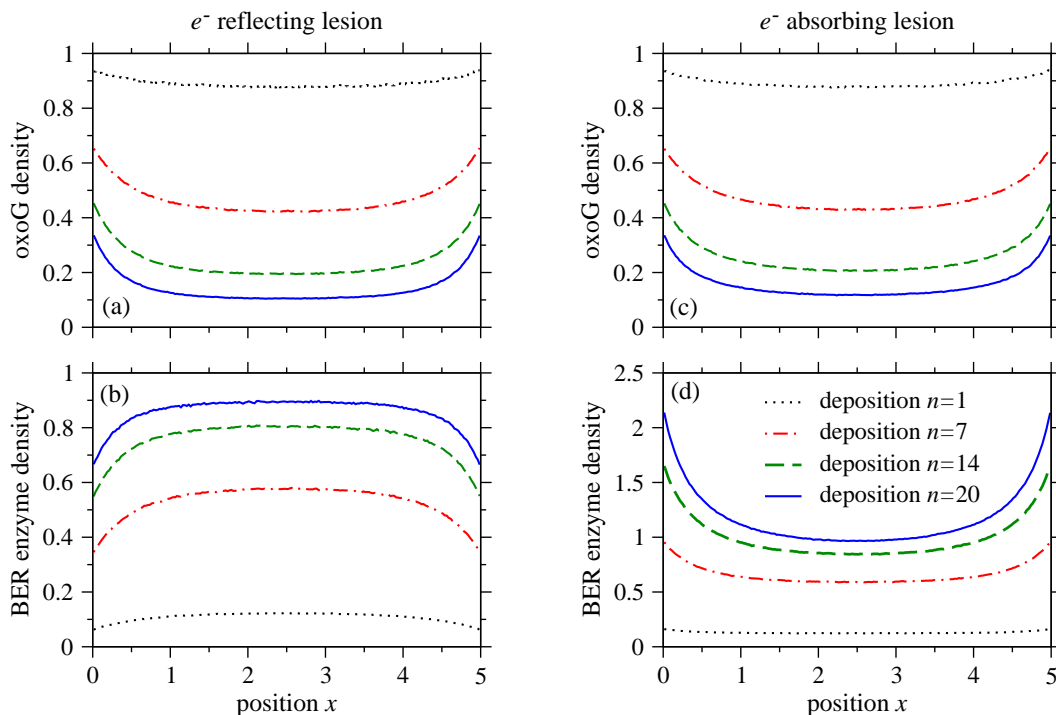


FIG. 7: Implicit-electron Monte-Carlo simulations of the evolution of mean guanine radical ((a) and (c)) and BER enzyme ((b) and (d)) density profiles after 1 (dotted), 7 (dot-dashed), 14 (dashed), and 20 (solid) enzyme depositions. (a) and (b) correspond to electron-reflecting lesions at $x = 0$ and $x = \Gamma = 5$, and (c) and (d) are for electron-absorbing lesions. Results were obtained from averaging 10^7 trials and using a flip rate of $f = 1$.

cals are annihilated. In the absence of any electron absorbers on the DNA, there can be no net increase in enzyme number, and the enzyme density in Fig. 7(b) eventually saturates to unity everywhere in the domain, identical to the initial oxoG density. Each guanine radical is eventually replaced by a BER enzyme, so the long-time BER enzyme density mimics the initial oxoG density.

In contrast, when the lesions are electron absorbing, there are always two permanent electron absorbers in the system. In this case, the number of enzymes can grow without bound, even when all the oxoGs are depleted.

Figure 8(a) shows how enzymes converge to electron absorbing lesions located at $x = 0$ and $x = \Gamma = 5$. At any given time, we label the m enzymes on the DNA according to their position E_i so that $0 < E_1 < E_2 < \dots < E_m < \Gamma$. Both the number of enzymes on the DNA, m , and their positions, E_i , are functions of n , the number of (attempted) depositions that have occurred. We plot the quantities $x_1 = \min(E_1, \Gamma - E_m)$, $x_2 = \min(E_2, \Gamma - E_{m-1})$ and $x_3 = \min(E_3, \Gamma - E_{m-2})$ as functions of deposition number n in Fig. 8(a). When fewer than 3 enzymes are adsorbed on the DNA, we define $x_i = \Gamma$, $i = 1, 2, 3$. From our simulations, we find the scaling

$$x_i \sim n^{-2/3} \text{ for } i = 1, 2, 3, \quad (22)$$

in the large n limit. For a BER enzyme to successfully excise a lesion, we assume that it has to be within a few

base pairs of it. We set the physical enzyme-lesion distance $X_1 \equiv x_1/\rho = 5a$, where a is the width of a base pair which we take to be 0.34 nm, and estimate n . Approximately 1 in 40,000 guanine bases are guanine radicals,³⁵ so $\rho = (160,000a)^{-1}$, and the number of attempted depositions required for the closest sticking enzyme to be within 5 base pairs of the lesion is $n \approx 6 \times 10^6$. If each deposition takes at least 0.0005 seconds,³⁹ this amounts to a total (minimum) search time of about 50 minutes. Although this is a significant reduction compared to the original 1D sliding search time discussed in the Introduction, it is likely that MutY locates lesions even more quickly through a combination of the CT mechanism and facilitated diffusion along the DNA strand.

The solid curve in Fig. 8(b) shows the total number of enzymes on the DNA as a function of the deposition number when the lesions at $x = 0$ and $x = 5$ are electron absorbing. Upon depletion of the guanine radicals (shown by the dotted curve dropping to $< 10^{-2}$), the enzyme number increases as $O(n^{1/3})$. The dashed curve in Fig. 8(b) shows the number of electrons absorbed by the lesion. Initially, this is less than the enzyme number since enzymes adsorb mainly by oxoG annihilation. However, as all the radicals are used up, the dashed curve asymptotes to the curve for the enzyme total, indicating that the net increase of enzymes on the DNA is due primarily to lesion-induced colocalization.

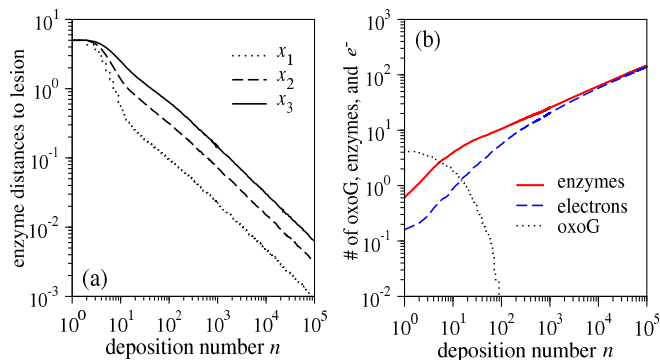


FIG. 8: (a) Convergence of repair enzymes to an electron absorbing lesion. The distance between the lesion and the closest, second closest and third closest enzymes (denoted by x_j , $j = 1, 2, 3$ respectively) scales as $O(n^{-2/3})$ for $n \gg 1$ where n is the deposition number. Results were obtained using $f = 1$ and by averaging over 5000 trials. (b) The total number of enzymes and guanine radicals on the DNA and the number of electrons absorbed by the lesion as a function of deposition number after averaging over 100 trials. The enzyme number scales as $O(n^{1/3})$ for $n \gg 1$. The dimensionless flip rate was $f = 1$, and the domain size was $\Gamma = 5$. There were initially 5 guanine radicals present.

Given that the enzyme-lesion distance scales as $O(n^{-2/3})$ for electron absorbing lesions, one can directly show that the number of enzymes on the DNA scales as $O(n^{1/3})$ through a simple argument. If the enzyme-lesion distance is $O(n^{-2/3})$ it takes $O(n^{2/3})$ attempts before an added enzyme lands closest to the lesion. When n is large, the enzyme-lesion distance is small and the electron released by the newly deposited enzyme will be absorbed. For every $O(n^{2/3})$ depositions, on average, one permanent adsorption occurs. Hence, for every $O(n)$ depositions, $O(n^{1/3})$ adsorptions occur.

While the convergence of CT enzymes towards lesions scales as $x_i \sim n^{-2/3}$, the convergence of passive enzymes (those that simply adsorb onto DNA without emitting electrons) scales as $x_i \sim n^{-1}$. The faster convergence of passive enzymes⁴⁰ is a consequence of linearly increasing the passive enzyme density on the DNA. The CT mechanism on the other hand, prevents the recruitment of large numbers of BER enzyme on the DNA at any given time with the total number scaling as $O(n^{1/3}) \ll O(n)$ for large n . Hence, although BER enzymes only colocalize near lesions (note the maxima in the enzyme density occur at the lesions in Fig. 7(d)), and the CT mechanism suppresses the wasteful build-up of enzymes in undamaged parts of the DNA.

IV. SUMMARY AND CONCLUSIONS

We developed a mathematical model for a proposed charge-transport mediated mechanism of Base Excision

Repair (BER) enzyme colocalization to DNA lesions. Enzymes adsorb and desorb through a charge transport (CT) mechanism^{4,5} which we model using a stochastic Broadwell process. Our main finding is that the CT mechanism concentrates repair enzymes at lesions provided the lesions are electron absorbing.

We first calculated enzyme sticking probabilities and self-desorption rates in the absence of lesions. Our results for an infinite, lesion free DNA, populated with guanine radicals, are summarized in Figs. 4 (which predicts the enzyme sticking probability) and 5 (which predicts the electron's mean conditional return time). For the deposition of a single enzyme onto an infinite DNA, the results are exact; for a given deposition rate per unit length, we expect the results to hold approximately providing the fraction of guanine radicals (oxoGs) annihilated is small. We also explored how enzymes colocalize to lesions using Monte-Carlo simulations. Enzymes were adiabatically deposited onto a circular DNA with a single lesion. We found that electron-absorbing lesions colocalize CT enzymes, and while electron-reflecting lesions do not (Fig. 7).

Simple facilitated diffusion is often unable to account for the fast search times observed in certain DNA-protein reactions.^{7,8} Cherstvy *et al.*¹⁸ state that under realistic conditions, facilitated diffusion cannot occur and propose that acceleration is achieved through the collective behavior of proteins. In the context of target search by enzymes, the CT mechanism complements facilitated diffusion models.^{11,16,17} The CT-mediated mechanism is one such example of collective behavior. Instead of basing the enzyme search problem on the time for a single protein to find its target, the CT mechanism relies on a collective build-up of enzyme density at the lesion. Hence, issues important in facilitated diffusion theories, such as the starting point of the enzyme relative to the lesion and the length of the DNA become irrelevant in the CT mechanism.

In the case where targets (lesions) are electron absorbing, we find that the maximum enzyme density always occurs at the permanent lesions and furthermore that the CT mechanism maintains a low density of enzymes far from lesions to suppress oxoGs, which are another form (albeit less permanent) of DNA damage. In fact, after an initial transient where all oxoGs are annihilated, the density of enzymes for most of the DNA will be of the order of the oxoG density, which is very low (about 1 in 160,000 base pairs). Subsequent enzyme depositions will colocalize only near the lesion. Our results show that although $n \sim 10^6$ (attempted) depositions are required for the concentration to build up to a sufficient level at the lesions in order for them to be excised, the number of enzymes actually adsorbed on the DNA is much less, at $O(n^{1/3}) \approx 100$. Although this is a significant reduction, it is still greater than the copy number of MutY (~ 20), so it is likely that the effects of 1D diffusion of MutY are important.⁶

When considering the collective behavior of enzymes,

one important constraint is that the number of BER enzymes available to participate in the search mechanism is fixed. The copy number for MutY, in particular, is about 20,³⁶ placing a bound on the total number of enzymes that can be successfully adsorbed on the DNA strand. Thus, the CT search mechanism is effective only if the number of oxoGs is not significantly greater than ~ 20 . Although guanine radicals absorb electrons, thereby seeding the adsorption of BER enzymes, too many radicals can deplete the reservoir of BER enzyme before they significantly concentrate to the lesions.

Although in our model, there are two modes of enzyme recruitment – oxoG-mediated and lesion-mediated (when the lesion is electron absorbing) – it is the latter that colocalizes enzymes to lesions. We re-emphasize that the initial recruitment by guanine radicals can only increase the enzyme density to a level that is of the order of the initial radical density. This density is far too low to ensure reliable excision of the lesion. However, upon subsequent depositions, enzymes rapidly colocalize and the accumulation is more focused.

Although our simple model successfully predicts colocalization of CT BER enzymes to electron-absorbing DNA lesions, it neglects many potentially important aspects. For example, BER enzymes are not point particles but have a finite size of about 10-15 base pairs. Random adsorption of finite sized particles has been studied³⁷ and could be used to enhance our current model. We also neglected the sliding of BER enzymes on DNA. Inclusion of finite size effects and enzyme sliding into our model is likely to decrease the search time to a lesion. The effect of other proteins on the DNA, besides BER enzymes, is also important. These proteins could physically prevent the adsorption of BER enzymes, absorb electrons emitted by BER enzymes or shield the lesion from electrons (or possibly all three). We currently do not know the effect of molecular crowding on the CT model, but this topic is discussed by Li *et al.*³⁸ One possible approach to studying these more subtle attributes is to develop and analyze them within coarse-grained, mass-action type models, in conjunction with Monte-Carlo simulations.

Acknowledgments

This work was supported by grants from the NSF (DMS-0349195) and the NIH (K25 AI41935). The authors thank J. Genereux, A. K. Boal and J. K. Barton for helpful discussions.

APPENDIX A: SOLUTION OF THE ONE-SIDED BROADWELL PROBLEM

Taking the Laplace transform of Eq. (6), we obtain

$$\frac{\partial \tilde{\mathbf{Q}}(x, s)}{\partial x} = \mathbf{M} \tilde{\mathbf{Q}}(x, s) + \begin{pmatrix} \delta(x - x_0) \\ 0 \end{pmatrix}, \quad (\text{A1})$$

where $\tilde{\mathbf{Q}}(x, s) = (\tilde{Q}_+(x, s), \tilde{Q}_-(x, s))^T$, $\tilde{Q}_\pm(x, s) \equiv \int_0^\infty Q_\pm(x, t) e^{-st} dt$ and

$$\mathbf{M} \equiv \begin{bmatrix} -(s + \mu + f) & f \\ -f & s + \mu + f \end{bmatrix}. \quad (\text{A2})$$

The solution to Eq. (A1), can be found in two separate regions $x > x_0$ and $x < x_0$ and matching the solutions with the appropriate jump conditions derived from integrating Eq. (A1) over an infinitesimal segment centered about x_0 :

$$\begin{aligned} \tilde{Q}_+(x_0^+, s) - \tilde{Q}_+(x_0^-, s) &= 1, \\ \tilde{Q}_-(x_0^+, s) - \tilde{Q}_-(x_0^-, s) &= 0. \end{aligned} \quad (\text{A3})$$

The general solution of Eq. (A1), $\tilde{\mathbf{Q}}(x, s; x_0, \ell)$, can be expressed in the form

$$\tilde{\mathbf{Q}}(x, s) = \begin{cases} A_< \begin{pmatrix} 1 \\ c_1 \end{pmatrix} e^{\lambda_1 x} + B_< \begin{pmatrix} 1 \\ c_2 \end{pmatrix} e^{\lambda_2 x}, & x < x_0, \\ A_> \begin{pmatrix} 1 \\ c_1 \end{pmatrix} e^{\lambda_1 x} + B_> \begin{pmatrix} 1 \\ c_2 \end{pmatrix} e^{\lambda_2 x}, & x > x_0, \end{cases} \quad (\text{A4})$$

where $\lambda_{1,2}(s)$, $c_{1,2}(s)$ are given by

$$\begin{aligned} \lambda_{1,2}(s) &= \pm \sqrt{(s + \mu)(s + \mu + 2f)}, \\ c_{1,2}(s) &= \frac{f}{s + \mu + f - \lambda_{1,2}(s)}. \end{aligned} \quad (\text{A5})$$

The constants $A_>$, $B_>$, $A_<$, and $B_<$ are obtained by imposing the Laplace Transformed boundary conditions $\tilde{Q}_+(0, s) = \tilde{Q}_-(\ell, s) = 0$, which come from Eq. (9), and the jump conditions (A3):

$$\begin{aligned} A_< &= \frac{c_1 c_2 e^{-(\lambda_1 + \lambda_2)x_0} [e^{\lambda_1 \ell + \lambda_2 x_0} - e^{\lambda_1 x_0 + \lambda_2 \ell}]}{(c_1 - c_2)(c_1 e^{\lambda_1 \ell} - c_2 e^{\lambda_2 \ell})}, \\ B_< &= \frac{c_1 c_2 e^{-(\lambda_1 + \lambda_2)x_0} [e^{\lambda_1 x_0 + \lambda_2 \ell} - e^{\lambda_1 \ell + \lambda_2 x_0}]}{(c_1 - c_2)(c_1 e^{\lambda_1 \ell} - c_2 e^{\lambda_2 \ell})}, \\ A_> &= \frac{c_2 e^{\lambda_2 \ell} [c_2 e^{-\lambda_1 x_0} - c_1 e^{-\lambda_2 x_0}]}{(c_1 - c_2)(c_1 e^{\lambda_1 \ell} - c_2 e^{\lambda_2 \ell})}, \\ B_> &= \frac{c_1 e^{\lambda_1 \ell} [c_1 e^{-\lambda_2 x_0} - c_2 e^{-\lambda_1 x_0}]}{(c_1 - c_2)(c_1 e^{\lambda_1 \ell} - c_2 e^{\lambda_2 \ell})}. \end{aligned} \quad (\text{A6})$$

APPENDIX B: LIMITING CASES OF THE BROADWELL MODEL

Upon eliminating P_- from Eqs. (1), P_+ satisfies

$$\frac{\partial^2 P_+}{\partial T^2} = -2(F + M)\frac{\partial P_+}{\partial T} + V^2\frac{\partial^2 P_+}{\partial X^2} - M^2 P_+. \quad (\text{B1})$$

Similarly, eliminating P_+ from Eqs. (1) gives Eq. (B1) but with P_+ replaced with P_- . Upon neglecting electron decay, $M = 0$, and Eq. (B1) simplifies to

$$\frac{\partial^2 P_+}{\partial t^2} + 2f\frac{\partial P_+}{\partial t} = \frac{\partial^2 P_+}{\partial x^2} \quad (\text{B2})$$

where we have used the nondimensionalization (5) and the non-dimensional flip rate $f = F/(\rho V)$. When $f \gg 1$, we neglect the first term in Eq. (B2) to obtain a diffusion equation with diffusivity $1/(2f)$. When $f \ll 1$, we neglect the second term to obtain a wave equation with unit wave speed. These limits correspond to a diffusive and ballistic electron motion respectively.

APPENDIX C: ADIABATIC APPROXIMATION

Since our stochastic analysis does not account for electron-electron interactions, we assume “adiabatic” deposition of BER enzymes. An adiabatic deposition of enzymes occurs when each enzyme is deposited sufficiently slowly so that the emitted electron completes its motion before the deposition of the next enzyme. At any given time, there is at most one traveling electron on the DNA.

Consider Figure 9: two enzymes are deposited on either side of a guanine radical with the left enzyme further away. For this example, assume that the electrons are always emitted toward the radical. In an adiabatic deposition, the deposition of the right enzyme occurs after the oxoG is annihilated. The final configuration consists of an adsorbed right enzyme and a desorbed left enzyme. In a non-adiabatic deposition, the right enzyme can be deposited before the annihilation of the oxoG. The final enzyme configuration depends critically on the time between the first and second depositions. If this time is long (a “late” second deposition), the oxoG is annihilated by the rightward electron and the final configuration is identical to the adiabatic case. If the inter-deposition time is short (an “early” second deposition), the leftward electron can annihilate the oxoG first and the final configuration corresponds to an adsorbed left enzyme and a desorbed right enzyme.

For a deposition to be adiabatic, the electron dynamics must be much faster than that of enzyme depositions:

$$\rho V, F \gg \frac{k_{\text{on}}}{\rho}, \quad (\text{C1})$$

where ρ is the density of guanine radicals and k_{on} is an intrinsic enzyme deposition rate per unit length of DNA.

Thus, the adiabatic limit arises when $\rho^2 V/k_{\text{on}} \rightarrow \infty$ and $\rho F/k_{\text{on}} \rightarrow \infty$, with $f = F/(\rho V)$ fixed (to keep the overall probabilities $\Pi_{\text{adsorb}}, \Pi_{\text{desorb}}$ unchanged in Eq. (11)). Note that f can still be small in an adiabatic deposition, as is the case in Fig. 9.

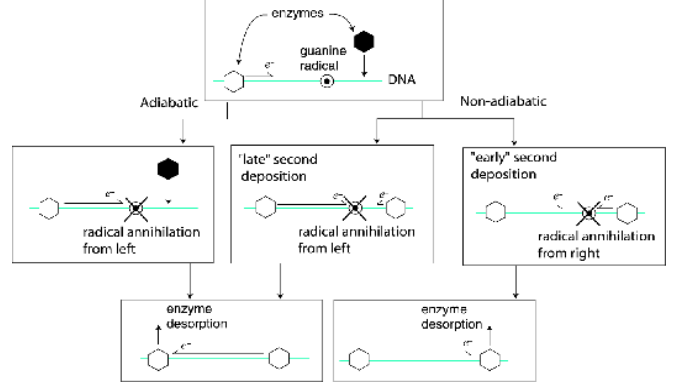


FIG. 9: Possible outcomes from an adiabatic and non-adiabatic deposition of a pair of repair enzymes. The left enzyme is always deposited first, but is further away from the guanine radical than the right one. The flip rate F satisfies $F \ll \rho V$ so that the electron motion is ballistic. The final configuration of a non-adiabatic deposition depends critically on the time between the first and second depositions.

APPENDIX D: GUANINE GAP DISTRIBUTION

Consider a lattice made up of n sites on which guanine radicals can randomly appear at a rate of Ω radicals per unit time T , per lattice site. Each lattice site can hold at most one guanine radical. The size of the *gap* between two guanine radicals is the number of empty sites between them. Let $N(m, T)$ denote the total number of gaps of size m (measured in lattice sites) at time T . Then $N(m, T)$ obeys³⁷

$$\frac{1}{\Omega} \frac{\partial N(m, T)}{\partial T} = 2 \sum_{m'=m+1}^n N(m', T) - mN(m, T). \quad (\text{D1})$$

We will take the continuum limit of Eq. (D1) when the number of sites becomes infinite, the guanine radicals become points on a line and the gap length becomes a continuous random variable, taking any value between 0 and ∞ . We aim to calculate the probability distribution function (PDF) of the gap length given a fixed average density of guanine radicals ρ .

Let L_0 be the total length of the lattice and a be the width of a single lattice site so that $L_0 = na$. Furthermore, the time taken for G guanines to appear on the lattice is T_0 , where $n\Omega T_0 = G$ and $\rho = G/L_0$.

Now we define dimensionless variables y, t and $p =$

$p(y, t)$ where

$$y = \rho am, \quad (\text{D2})$$

$$t = T/T_0, \quad (\text{D3})$$

$$p = N/(n\Omega T) = N/(Gt). \quad (\text{D4})$$

Note that $0 < y < \infty$ and that for large G , Gt is approximately the total number of gaps at time t ; hence p in Eq. (D4) is the fraction of gaps that have size N at time t .

The desired continuum limit is now obtained by taking $n \rightarrow \infty$, $a\rho \rightarrow 0$ so that y in Eq. (D2) becomes a continuous variable ranging from 0 to ∞ , and $G, L_0 \rightarrow \infty$: the number of radicals that appear and the DNA length become infinite in such a way that $\rho \equiv G/L_0$ stays a constant. When these limits are taken, $p(y, t)$ becomes the probability of finding a gap of length y at time t and $\int_0^\infty p(y, t) dy = 1$. Upon setting $q(y, t) = tp(y, t)$, we obtain the integro-differential equation

$$\frac{\partial q}{\partial t} = 2 \int_y^\infty q(y', t) dy' - yq(y, t). \quad (\text{D5})$$

The Laplace transform in t of Eq. (D5) is

$$s\tilde{q}(y, s) = 2 \int_y^\infty \tilde{q}(y', s) dy' - y\tilde{q}(y, s), \quad (\text{D6})$$

where $\tilde{q}(y, s) = \int_0^\infty e^{-st} q(y, t) dt$ and we have used the initial condition $p(y, 0) = 0$. Differentiating Eq. (D6) with respect to y gives

$$\frac{d\tilde{q}(y, s)}{dy} + \frac{3\tilde{q}(y, s)}{(y+s)} = 0, \quad (\text{D7})$$

which is solved by $\tilde{q}(y, s) = A(s)/(y+s)^3$. To determine the integration constant $A(s)$, we take the $y \rightarrow 0$ limit of Eq. (D5) to obtain

$$\left. \frac{\partial q}{\partial t} \right|_{y=0} = 2 \int_0^\infty q(y', t) dy' = 2t, \quad (\text{D8})$$

where the last equality arises from the normalization of $p(y, t)$. The Laplace transform of Eq. (D8) gives $\tilde{q}(0, s) = 2/s^3$. Hence, $\tilde{q}(y, s) = 2/(y+s)^3$ resulting in $q(y, t) = t^2 e^{-yt}$ and $p(y, t) = te^{-yt}$. Therefore, if Y is the non-dimensionalized gap length at $t = 1$, we find

$$\text{Prob}(y \leq Y \leq y + dy) = e^{-y} dy. \quad (\text{D9})$$

-
- * pakwing@caltech.edu
† tomchou@ucla.edu
- ¹ S. D. Bruner, D. P. G. Norman, and G. L. Verdine, *Nature* **403**, 859 (2000).
 - ² H. M. Nash, S. D. Bruner, O. D. Schärer, T. Kawate, T. A. Addona, E. Spooner, W. S. Lane, and G. L. Verdine, *Current biology* **6**, 968 (1996).
 - ³ S. S. Parikh, C. D. Mol, and J. A. Tainer, *Structure* **5**, 1543 (1997).
 - ⁴ E. Yavin, A. K. Boal, E. D. A. Stemp, E. M. Boon, A. L. Livingston, V. L. O'Shea, S. S. David, and J. K. Barton, *Proceedings of the National Academy of Science* **102**, 3546 (2005).
 - ⁵ E. M. Boon, A. L. Livingston, M. H. Chmiel, S. S. David, and J. K. Barton, *Proceedings of the National Academy of Science* **100**, 12543 (2003).
 - ⁶ P. C. Blainey, A. M. van Oijen, A. Banerjee, G. L. Verdine, and X. S. Xie, *Proceedings of the National Academy of Science* **103**, 5752 (2006).
 - ⁷ A. D. Riggs, S. Bourgeois, and M. Cohn, *J. Mol. Biol.* **53**, 401 (1970).
 - ⁸ A. D. Riggs, H. Suzuki, and S. Bourgeois, *J. Mol. Biol.* **53**, 401 (1970).
 - ⁹ O. G. Berg, R. B. Winter, and P. H. von Hippel, *Biochemistry* **20**, 6929 (1981).
 - ¹⁰ R. B. Winter, O. G. Berg, and P. H. von Hippel, *Biochemistry* **20**, 6961 (1989).
 - ¹¹ P. H. von Hippel and O. G. Berg, *J. Biol. Chem.* **264**, 675 (1989).
 - ¹² O. G. Berg and P. H. von Hippel, *J. Mol. Biol.* **193**, 723 (1987).
 - ¹³ L. A. Mirny, *Nature Physics* **4**, 93 (2008).
 - ¹⁴ Z. Wunderlich and L. A. Mirny, *Nucleic Acids Research* **36**, 3570 (2008).
 - ¹⁵ K. Klenin, H. Merlitz, J. Longowski, and C.-X. Wu, *Phys. Rev. Lett.* **96**, 018104 (2006).
 - ¹⁶ M. Slutsky and L. A. Mirny, *Biophys. J.* **87**, 4021 (2004).
 - ¹⁷ T. Hu, A. Y. Grosberg, and B. I. Shklovskii, *Biophys. J.* **80**, 2731 (2006).
 - ¹⁸ A. G. Cherstvy, A. B. Kolomeisky, and A. A. Kornyshev, *J. Phys. Chem.* **112**, 4741 (2008).
 - ¹⁹ S. E. Halford and J. F. Marko, *Nucleic Acids Res.* **32**, 3040 (2004).
 - ²⁰ Y. M. Wang, R. H. Austin, and E. C. Cox, *Phys. Rev. Lett.* **97**, 048302 (2006).
 - ²¹ C. Loverdo, O. Bénichou, M. Moreau, and R. Voituriez, *Nature Physics* **4**, 134 (2008).
 - ²² A. K. Boal, E. Yavin, O. A. Lukianova, V. L. O'Shea, S. S. David, and J. K. Barton, *Biochemistry* **44**, 8397 (2005).
 - ²³ B. Giese, *Annu. Rev. Biochem.* **71**, 51 (2002).
 - ²⁴ G. B. Schuster, *Acc. Chem. Res.* **33**, 253 (2000).
 - ²⁵ N. J. Turro and J. K. Barton, *J. Biol. Inorg. Chem.* **3**, 201 (1998).
 - ²⁶ C. J. Murphy, M. R. Arkin, Y. Jenkins, N. D. Ghatlia, S. H. Bossman, N. J. Turro, and J. K. Barton, *Science* **262**, 1025 (1993).
 - ²⁷ K. A. Eriksen, *Theoretical Biology and Medical Modelling* **2**, 15 (2005).
 - ²⁸ S. Redner, *A guide to first-passage processes* (Cambridge University Press, 2001).
 - ²⁹ D. J. Bicout, *Phys. Rev. E* **56**, 6656 (1997).
 - ³⁰ J. E. Broadwell, *Phys. Fluids* **7**, 1243 (1964).

- ³¹ J. E. Broadwell, *J. Fluid Mech.* **19**, 401 (1964).
- ³² A. J. Christlieb, J. A. Rossmannith, and P. Smereka, *Comm. Math. Sci.* **2**, 443 (2004).
- ³³ M. R. D’Orsogna and J. Rudnick, *Phys. Rev. E* **66**, 041804 (2002).
- ³⁴ R. Bruinsma, G. Gruner, M. R. D’Orsogna, and J. Rudnick, *Phys. Rev. Lett.* **85**, 4393 (2000).
- ³⁵ H. J. Helbock, K. B. Beckman, M. K. Shigenaga, P. B. Walter, A. A. Woodall, H. C. Yeo, and B. N. Ames, *Proc. Natl. Acad. Sci. USA* **95**, 288 (1998).
- ³⁶ H. Bai and A.-L. Lu, *J. Bacteriol.* **189**, 902 (2007).
- ³⁷ M. R. D’Orsogna and T. Chou, *J. Phys. A* **38**, 531 (2005).
- ³⁸ G.-W. Li, O. G. Berg, and J. Elf, arXiv:0809.1063 (2008).
- ³⁹ For *E. Coli*, the maximum deposition rate can be obtained by assuming a nucleoid radius of approximately $b \approx 0.3\mu\text{m}$. Upon assuming a MutY diffusivity of $D \sim 3 \times 10^{-7}\text{cm}^2/\text{s}$, the Debye-Smoluchowski estimate is $k_{\text{on}} \sim 4\pi Db \approx 6 \times 10^{10} \text{M}^{-1}\text{s}^{-1}$. For MutY concentration of $C \approx 20 \text{enzymes}/\text{fL}$, the average time between depositions is $(kC)^{-1} \approx 0.0005\text{s}$.
- ⁴⁰ While passive enzymes converge more quickly to enzymes when measured in terms of the deposition number n , CT repair enzymes converge more quickly when measured in terms of the number of adsorptions $m = O(n^{1/3})$. In fact, the enzyme-lesion distance for repair enzymes scales as $O(n^{-2/3}) = O(m^{-2})$ compared to $O(m^{-1})$ for passive enzymes with $m = n$ (every deposition results in an adsorption).